Supplementary Material for "Role of the crystal lattice structure in the selection of fracture toughness"

Thuy Nguyen, Daniel Bonamy

Supplementary Material for "Role of the crystal lattice structure in the selection of fracture toughness"

Thuy Nguyen[1,2] and Daniel Bonamy[1,*]

[1] *Service de Physique de l'Etat Condensée, CEA, CNRS, Université Paris-Saclay, CEA Saclay 91191 Gif-sur-Yvette Cedex, France*

[2] *EISTI, Université Paris-Seine, Avenue du Parc, 95000 Cergy Pontoise Cedex, France*

I. SCALAR ANTIPLANE ELASTICITY PROBLEM – DETERMINATION OF YOUNG MODULUS IN THE DIFFERENT LATTICE GEOMETRIES

The 2D fuse networks considered here are electrical analogs of a scalar antiplane elasticity problem so that the local voltage, $u(x,y)$, maps to the out-of-plane displacement, $\mathbf{u} = u(x,y)\mathbf{e}_z$. To compute Young's modulus, we then consider a given node i and its connected neighbors j. The components of the stress tensor associated to i is given by[1]:

$$\sigma = \frac{1}{2A_i}\sum_j (\mathbf{r}_j - \mathbf{r}_i) \times \mathbf{F}_{ji}, \tag{S1}$$

where A_i is the area of the Voronoi polyedra associated with node i, $\mathbf{r}_i$ and $\mathbf{r}_j$ the position of nodes i and j, and $\mathbf{F}_{ji}$ the force applied by node j on node i. Here, $\mathbf{F}_{ji} = F_{ji}\mathbf{e}_z$, and $F_{ji} = (u_j - u_i)$ where u_i refers to the voltage at node i (the fuse conductance is recalled to be one). As a result, only σ_{xz} and σ_{yz} are different from zero; they are given by:

$$\sigma_{xz} = \frac{1}{2A_i}\sum_j (v_j - v_i)(\mathbf{r}_j - \mathbf{r}_i)\cdot\mathbf{e}_x \text{ and } \sigma_{yz} = \frac{1}{2A_i}\sum_j (v_j - v_i)(\mathbf{r}_j - \mathbf{r}_i)\cdot\mathbf{e}_y \tag{S2}$$

Considering now the strain tensor, only the components ϵ_{xz} and ϵ_{yz} are different from zero. Then, $v_j - v_i$ can be written as: $v_j - v_i = 2\epsilon_{xz}(\mathbf{r}_j - \mathbf{r}_i)\cdot\mathbf{e}_x + 2\epsilon_{yz}(\mathbf{r}_j - \mathbf{r}_i)\cdot\mathbf{e}_y$. Introducing this expression into Eq. S2 leads to:

$$\sigma_{xz} = \frac{1}{A_i}\epsilon_{xz}\sum_j (x_j - x_i)^2 \quad \text{and} \quad \sigma_{yz} = \frac{1}{A_i}\epsilon_{yz}\sum_j (y_j - y_i)^2 \tag{S3}$$

Finally, since in this 2D scalar elastic problem, $\sigma_{xz} = E\epsilon_{xz}$ and $\sigma_{yz} = E\epsilon_{yz}$, one gets the following expression for Young's modulus E:

$$E = \frac{1}{A_i}\sum_j (x_j - x_i)^2 = \frac{1}{A_i}\sum_j (y_j - y_i)^2 \tag{S4}$$

In the square, triangular, and honeycomb lattices studied here:

- A_i is 1, $\sqrt{3}/2$ and $3\sqrt{3}/4$, respectively;
- the sequence $x_j - x_i$ is $\{1, 0, -1, 0\}$, $\{1, 1/2, -1/2, -1, -1/2, 1/2\}$ and $\{\sqrt{3}/2, 0, -\sqrt{3}/2\}$, respectively;
- the sequence $y_j - y_i$ is $\{0, 1, 0, -1\}$, $\{0, \sqrt{3}/2, \sqrt{3}/2, 0, -\sqrt{3}/2, -\sqrt{3}/2\}$ and $\{-1/2, 1, -1/2\}$, respectively.

Numerical application of Eq. S4 with the values above provides the values reported in the first column of Tab. 1 (main text).

* Daniel.Bonamy@cea.fr

II. SCALAR ANTIPLANE ELASTICITY PROBLEM – WILLIAMS'S EXPANSION FOR THE DISPLACEMENT/VOLTAGE FIELD

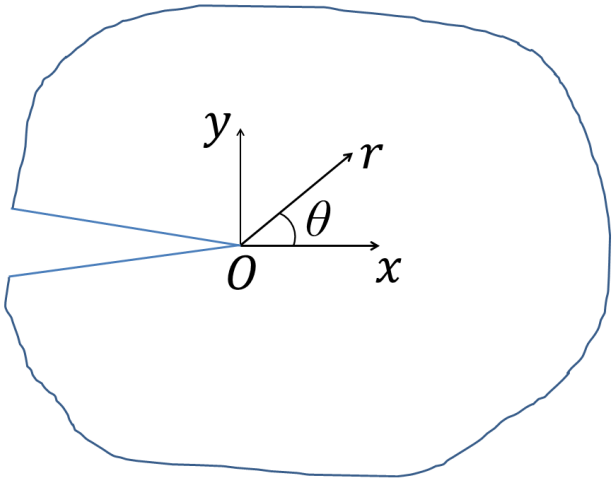

FIG. S1. Slit crack embedded in a 2D plate: sketch and notations

In the 2D antiplane scalar elasticity problem considered here, the equilibrium equation writes:

$$\triangle u = 0 \tag{S5}$$

Consider a straight slit crack embedded in the medium [Fig. S1], locate the origin at the crack tip, and recast Eq. S5 in polar coordinates:

$$\frac{\partial^2 u}{\partial r^2} + \frac{1}{r}\frac{\partial u}{\partial r} + \frac{1}{r^2}\frac{\partial^2 u}{\partial \theta^2} = 0 \tag{S6}$$

The condition of free surfaces along the crack imposes:

$$\sigma_{yz}(r, \pm\pi) = \mu \frac{\partial u}{\partial r}(r, \pm\pi) = 0, \tag{S7}$$

where μ is the shear modulus: $\mu = 2E$. Let us seek solutions of the form $u(r, \theta) = r^\lambda f(\theta, \lambda)$. Equation S6 yields:

$$f''(\theta) + \lambda f(\theta) = 0, \tag{S8}$$

whose solutions take the form $f(\theta) = A\cos(\lambda\theta) + B\sin(\lambda\theta)$. Hence, the elementary solutions for $u(r, \theta)$ write $u(r, \theta) = r^\lambda(A\cos(\lambda\theta) + B\sin(\lambda\theta))$. The problem symmetry imposes $u_z(r, \theta) = u_z(r, -\theta)$, hence $A = 0$. At this stage, the elementary solutions for u write:

$$u(r, \theta) = Br^\lambda \sin(\lambda\theta) \tag{S9}$$

Boundary conditions (Eq. S7) now impose $r^{\lambda-1}B\cos(\pm\pi(\lambda - 1)) = 0$, yielding $\lambda = n/2$ with $n = \pm1, \pm3, \pm5, ...$ Equation S9 now writes:

$$u(r, \theta) = \sum_{n=\pm1,\pm3,...} a_n r^{n/2} \sin\frac{n\theta}{2} \tag{S10}$$

Finally, continuity at the crack tip imposes $u(r = 0, \theta) = 0$; hence $n \geq 0$ and Eq. S10 takes the form of Eqs. 3 and 4 (main text).

III. SCALAR ANTIPLANE ELASTICITY PROBLEM – DETERMINATION OF CRACK-TIP MIS-POSITIONING WITH AN ARBITRARY NUMBER OF NODES

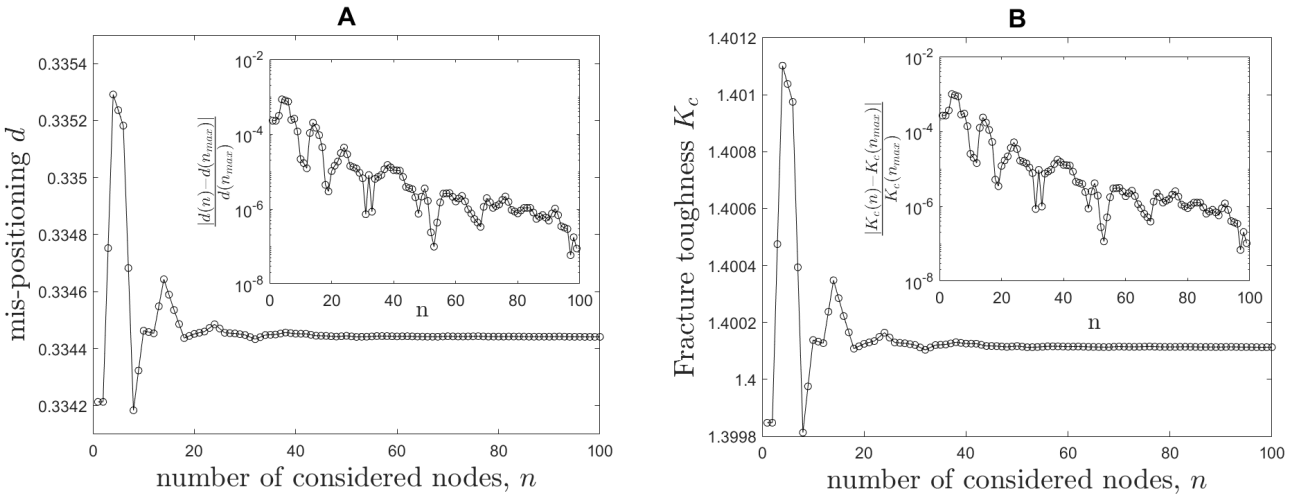

FIG. S2. Determination of fracture toughness with an arbitrary number of nodes. (a) Effect of the number of considered nodes, n, onto the determined value for mispositioning, d in the scalar elastic problem. Here, d is computed using Eq. S16. The considered nodes $\mathbf{P}$ are those the closest to the initial frame origin $\mathbf{O}$, located at the center of the next fuse to burn. (b) Variation with n of the fracture toughness, K_c obtained by inserting these values for d in Eq. 6 (main text). In both panels, the insets show the relative variation with respect to the last values $d(n_{max})$ and $K_c(n_{max})$, with $n_{max} = 100$.

As in main text, the crack tip is first placed *ad hoc* at the center of the next bond about to break, $\mathbf{O}$, and the reference frame is placed at this location. Let us consider a set of nodes, $\mathbf{P}$, in the vicinity of this crack tip, and call $\mathbf{P}_i$ their nearest neighbors, that is the nodes connected to $\mathbf{P}$ via an element. In the limit of large lattices ($L \to \infty$) the voltage at $\mathbf{P}$ writes:

$$u(\mathbf{P}) = a_{-1}\Phi^{III}_{-1}(r_{\mathbf{P}}, \theta_{\mathbf{P}}) + a_1\Phi^{III}_1(r_{\mathbf{P}}, \theta_{\mathbf{P}}), \tag{S11}$$

where $(r_{\mathbf{P}}, \theta_{\mathbf{P}})$ are the polar coordinates of point $\mathbf{P}$ and $\Phi^{III}_n(r, \theta)$ are the elementary functions provided in Eq. 4 (main text). The voltage at $\mathbf{P}_i$ takes the very same form. Kirchhoff law then imposes $\sum_i (u(\mathbf{P}) - u(\mathbf{P}_i)) = 0$ at each node $\mathbf{P}$. This leads:

$$a_{-1}S_{-1}(\mathbf{P}, \mathbf{P}_i) + a_1 S_1(\mathbf{P}, \mathbf{P}_i) = 0, \tag{S12}$$

where:

$$S_n(\mathbf{P}, \mathbf{P}_i) = \sum_i \left(\Phi^{III}_n(r_{\mathbf{P}}, \theta_{\mathbf{P}}) - \Phi^{III}_n(r_{\mathbf{P}_i}, \theta_{\mathbf{P}_i})\right). \tag{S13}$$

To first order in a_{-1}/a_1, the mispositioning is given by $d = 2a_{-1}/a_1$. Hence, Eq. S12 writes:

$$dS_{-1}(\mathbf{P}, \mathbf{P}_i) + 2S_1(\mathbf{P}, \mathbf{P}_i) = 0. \tag{S14}$$

The value of d should satisfy at best Eq. S14 for all $\mathbf{P}$. As such, it should minimize the function:

$$f(d) = \sum_{\mathbf{P}} \left(dS_{-1}(\mathbf{P}, \mathbf{P}_i) + 2S_1(\mathbf{P}, \mathbf{P}_i)\right)^2 \tag{S15}$$

This is satisfied for $f'(d) = 0$, so:

$$d = -2\frac{\sum\limits_{\mathbf{P}} S_{-1}(\mathbf{P},\mathbf{P}_i)S_1(\mathbf{P},\mathbf{P}_i)}{\sum\limits_{\mathbf{P}} S^2_{-1}(\mathbf{P},\mathbf{P}_i)} \tag{S16}$$

This equation provides a generalization of Eq. 5 (main text) in the case where several nodes $\mathbf{P}$ are considered. Figure S2(a) shows how d evolves with the number n of nodes considered (sorted by distance from $\mathbf{O}$). Very rapidly, d becomes independent of n; the relative variation in d is found to be smaller than 10^{-4} as soon as n is larger than 20. The fracture toughness is subsequently deduced by applying Eq. 6 (main text), after having shifted the frame origin over d. Its variation with n is plotted in Fig. S2(b).

IV. SCALAR ANTIPLANE ELASTICITY PROBLEM – ITERATIVE PROCEDURE TO DETERMINE THE CRACK-TIP MIS-POSITIONING

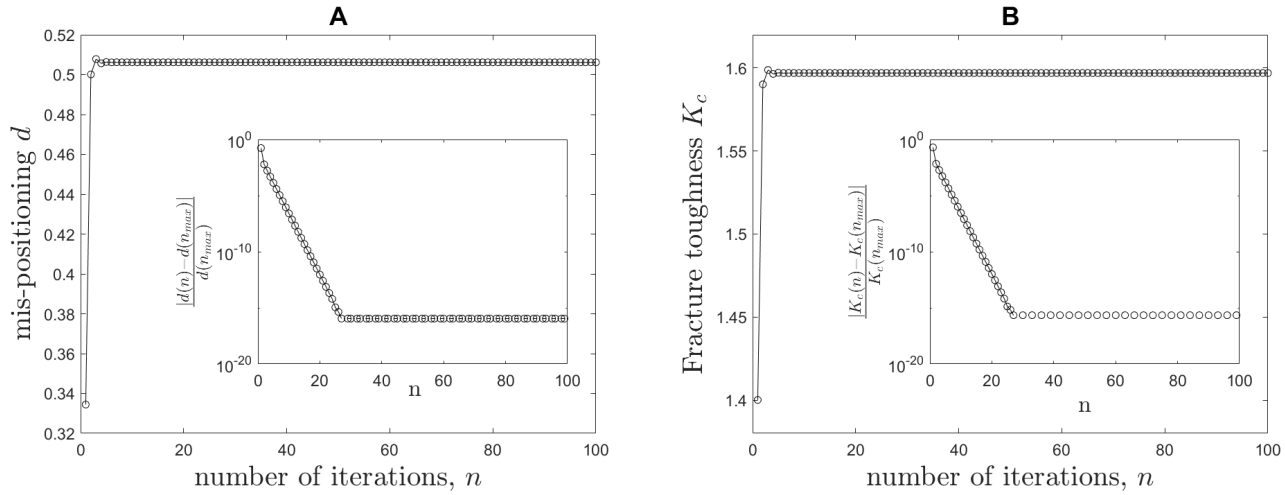

FIG. S3. Determination of fracture toughness with an arbitrary number of nodes. (a) Effect of the number of iterations, n, onto the determined value for mispositioning, d. At each iteration, d is computed using Eq. S16 by considering the 100 nodes the closest from the crack tip position as determined at the previous iteration. The initial crack tip position is placed at the middle $\mathbf{O}$ of the next fuse to burn. (b) Variation with n of the fracture toughness, K_c obtained by inserting these values for d in Eq. 6 (main text). In both panels, the insets show the relative variation with respect to the last values $d(n_{max})$ and $K_c(n_{max})$, with $n_{max} = 100$.

As in main text, the crack tip is first placed *ad-hoc* at the center of the next bond about to break and the reference frame, $\mathbf{O}$ is placed at this location. The tip mispositioning is then computed using Eq. S16 by considering the $n = 100$ nodes the closest to $\mathbf{O}$, denoted $\mathbf{P}$. The frame origin $\mathbf{O}$ is then shifted to the new position $\mathbf{O} \to \mathbf{O} - d\mathbf{e}_x$ with $\mathbf{e}_x$ parallel to the crack. The mis-positioning is computed again and the frame origin is switched again. The procedure is repeated 100 times. Figure S3(a) shows how d evolves with the number n of iterations. After 6 iterations, the relative variation in d is found to be smaller than 10^{-4}. The fracture toughness is subsequently deduced by applying Eq. 6 (main text) after having shifted the frame origin over the final d. Its variation with n is plotted in Fig. S3(b).

V. PLANE STRESS TENSORIAL ELASTICITY – DETERMINATION OF CRACK TIP MIS-POSITIONING WITHIN A BIDIMENSIONAL CRYSTAL

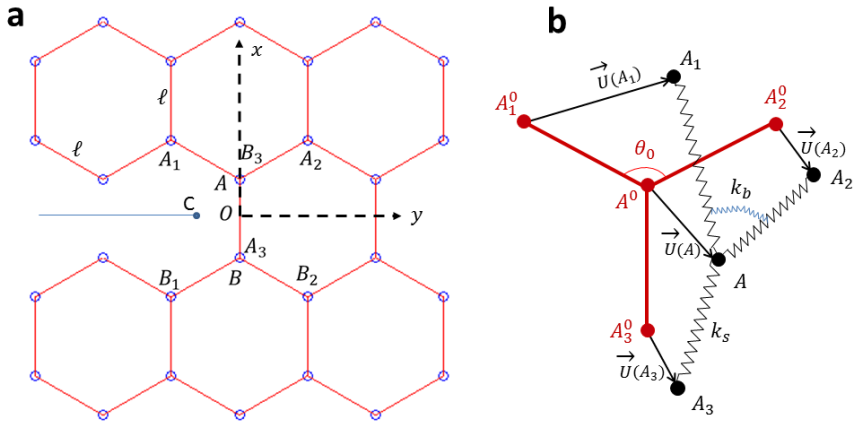

FIG. S4. Lattice geometry and atomistic deformation modes. (a) The honeycomb lattice geometry is chosen as an illustration; such a geometry is that presented by graphene. Each atom is bonded to three nearest-neighbors at equal distance ℓ, so that the bond angle at rest is $\theta_0 = 2\pi/3$. A straight slit crack is introduced in the lattice by withdrawing the bonds along a horizontal line in the middle. Atoms $\mathbf{A}$ and $\mathbf{B}$ denote the edges of the next bond about to break, $\mathbf{A}_i$ and $\mathbf{B}_i$ are the atoms connected to them. The frame is chosen so that $\mathbf{e}_x$ is parallel to the crack, and $\mathbf{e}_y$ is perpendicular to it. The frame origin $\mathbf{O}$ is placed in the middle of the bond $\mathbf{AB}$. The true position of the continuum-level scale crack tip is labeled $\mathbf{C}$. The mispositioning d is the distance $|\mathbf{CO}|$. (b) Bond stretching and bending modes involved in the deformation of a bidimensional crystal at the atomistic scale. Superscript ^{0} denotes the reference lattice configuration while no superscript indicates the atom position after the lattice deformation: The displacements at $\mathbf{A}$ and $\mathbf{A}_i$ due to the elastic deformations write $\mathbf{u}(\mathbf{A}) = \mathbf{A}^0\mathbf{A}$ and $\mathbf{u}(\mathbf{A}_i) = \mathbf{A}_i^0\mathbf{A}_i$. k_s and k_b refer to the bond stretching and bending stiffness, respectively.

Let us consider a two-dimensional crystal embedding a straight slit crack as depicted in Fig. S4(a). $\mathbf{e}_x$ is defined parallel to the crack, and $\mathbf{e}_y$ is perpendicular to it. For sake of simplicity, the bond angle θ_0 and bond length ℓ are assumed to be the same for all atoms. Let us now assume that the lattice is very large ($L \to \infty$) and loaded remotely under pure tension (mode I fracture).

A. *Williams expansion in plane stress conditions*

As shown by Williams [2], the displacement field $u(z)$ takes the form:

$$u(z) = \sum_{n\geq 0} a_n \Phi_n^I(z), \tag{S17}$$

Complex notations are used here: The position of a material point is represented by a complex number $z = x + iy$ or in polar coordinates $z = re^{i\theta}$. Accordingly, u (and Φ_n^I) are complex numbers, the real and imaginary part of which provides the component along x and y, respectively. For the following, it is worth to note that the inner product $\mathbf{u}\cdot\mathbf{v}$ of two vectors and the vectorial product $\mathbf{u}\times(\mathbf{v}\times\mathbf{w})$ write, within this complex notations:

$$\begin{aligned}\mathbf{u}\cdot\mathbf{v} &\equiv \mathrm{Re}\{z_u\,\overline{z}_v\},\\ \mathbf{u}\times(\mathbf{v}\times\mathbf{w}) &\equiv i\,\overline{z}_u\;\mathrm{Im}\{\overline{z}_v\,z_w\}\text{'}\end{aligned} \tag{S18}$$

where $\overline{z}$ is the conjugate of z, $\mathrm{Re}\{z\}$ is its real part, and $\mathrm{Im}\{z\}$ is its imaginary part.

In Eq. S17, the prefactors a_n are real numbers. The elementary solutions $\Phi_n^I(z)$ are generic and write [3]:

$$\Phi_n^I(z) = r^{n/2}\left(\kappa e^{in\theta/2} - \frac{n}{2}e^{i(4-n)\theta/2} + \left(\frac{n}{2}+(-1)^n\right)e^{-in\theta/2}\right), \tag{S19}$$

where $\kappa = (3-\nu)/(1+\nu)$ for the plane stress conditions encountered in two-dimensional crystals; ν is the Poisson ratio. The term $n=1$ is the usual square root singular term of LEFM where a_1 relates to the (mode I) stress intensity factor K as:

$$a_1 = \frac{K(1+\nu)}{E\sqrt{2\pi}}, \tag{S20}$$

B. *First order approximation of the crack tip mis-positioning*

As for the scalar elastic problem addressed in the main text, the difficulty is to place properly the frame origin at the true tip of the continuum-level scale crack in a lattice which is discrete at the atomistic scale. As a first guess, we place it at the middle, $\mathbf{O}$, of the bond about to break [Fig. S4(a)]. By doing so, we make a small error, d, in the positioning. This introduces an additional super-singular term $a_{-1}\Phi_{-1}^I(z)$ in Eq. S17, where $a_{-1}/a_1 = d/2$ [3].

To determine a_{-1}/a_1, we consider the force balance at one of the two edge atoms of the bond about to break, $\mathbf{A}$ [Fig. S4(a)]. At the discrete atomistic scale, elastic deformations are accommodated via two lattice deformation modes, bond stretching and bond bending. They are examined successively.

The force applying to $\mathbf{A}$ due to the stretching of the bond connecting $\mathbf{A}$ to its neighbors $\mathbf{A}_p$ writes:

$$\mathbf{F}_s(\mathbf{A}_p \to \mathbf{A}) = k_s\Delta\ell\,\mathbf{e}_{\mathbf{AA}_p}, \tag{S21}$$

where k_s is the bond stretching stiffness and $\mathbf{e}_{\mathbf{AA}_p}$ is the unit vector parallel to $\mathbf{A}^0\mathbf{A}_p^0$; here and thereafter, superscript ^{0} denotes the point position in the reference state, in absence of any elastic deformations. $\Delta\ell = |\mathbf{AA}_p| - |\mathbf{A}^0\mathbf{A}_p^0|$ is the length increment due to the displacements $\mathbf{u}(\mathbf{A})$ and $\mathbf{u}(\mathbf{A}_p)$ at $\mathbf{A}$ and $\mathbf{A}_p$. Since these displacements are infinitesimal, only the first order terms in $\mathbf{u}$ are kept, leading to:

$$\Delta\ell = \frac{1}{\ell}\mathbf{AA_p}\cdot(\mathbf{u}(\mathbf{A}_p) - \mathbf{u}(\mathbf{A})), \tag{S22}$$

using the complex notations defined previously, Eq. S21 becomes:

$$\mathbf{F}_s(\mathbf{A}_p \to \mathbf{A}) = \frac{k_s}{\ell^2}\,\mathrm{Re}\{(u(z_{\mathbf{A}_p}) - u(z_{\mathbf{A}}))(\overline{z}_{\mathbf{A}_p} - \overline{z}_{\mathbf{A}})\}(z_{\mathbf{A}_p} - z_{\mathbf{A}}). \tag{S23}$$

The force applying to $\mathbf{A}$ due to the bending of bonds connecting $\mathbf{A}$ to $\mathbf{A}_p$ and $\mathbf{A}$ to $\mathbf{A}_q$ [Fig. S4(b)] writes:

$$\mathbf{F}_b(\{\mathbf{A}_p,\mathbf{A}_q\} \to \mathbf{A}) = -\frac{k_b}{\ell}\Delta\theta\,\mathbf{e}^{\perp}_{\mathbf{A}_p\mathbf{A}_q}. \tag{S24}$$

where k_b is the bond bending stiffness and $\mathbf{e}^{\perp}_{\mathbf{A}_p\mathbf{A}_q}$ is the unit vector perpendicular to $\mathbf{A_p^0A_q^0}$: $\mathbf{e}^{\perp}_{\mathbf{A}_p\mathbf{A}_q} = (1/\ell^3)\mathbf{A_p^0A_q^0}\times(\mathbf{A^0A_p^0}\times\mathbf{A^0A_q^0})$. $\Delta\theta$ is the change in the bond angle due to the displacements $\mathbf{u}(\mathbf{A})$, $\mathbf{u}(\mathbf{A}_p)$ and $\mathbf{u}(\mathbf{A}_q)$. To first order in $\mathbf{u}$, it writes:

$$\begin{aligned}\Delta\theta &= -\frac{1}{\sin\theta_0}(\cos\theta-\cos\theta_0)\\ &= \frac{1}{\ell^2\sin\theta_0}\mathbf{A^0A^0_p}\cdot\Big(\mathbf{u}(\mathbf{A}_p)\cos\theta_0-\mathbf{u}(\mathbf{A}_q)+(1-\cos\theta_0)\mathbf{u}(\mathbf{A})\Big)\\ &\quad+\frac{1}{\ell^2\sin\theta_0}\mathbf{A^0A^0_q}\cdot\Big(\mathbf{u}(\mathbf{A}_q)\cos\theta_0-\mathbf{u}(\mathbf{A}_p)+(1-\cos\theta_0)\mathbf{u}(\mathbf{A})\Big),\end{aligned} \tag{S25}$$

And, using the complex notations defined previously, Eq. S24 becomes:

$$\begin{aligned}\mathbf{F}_b(\{\mathbf{A}_p,\mathbf{A}_q\}\to\mathbf{A}) = &-\frac{k_b}{\ell^6\sin\theta_0}i\times\Big(\overline{z}_{\mathbf{A}_q}-\overline{z}_{\mathbf{A}_p}\Big)\times\mathrm{Im}\Big\{(\overline{z}_{\mathbf{A}_p}-\overline{z}_{\mathbf{A}})(z_{\mathbf{A}_q}-z_{\mathbf{A}})\Big\}\\ &\times\mathrm{Re}\Big\{\left(\overline{z}_{\mathbf{A}_p}-\overline{z}_{\mathbf{A}}\right)\left(u(z_{\mathbf{A}_p})\cos\theta_0-u(z_{\mathbf{A}_q})+(1-\cos\theta_0)u(z_{\mathbf{A}})\right)\\ &\quad+\left(\overline{z}_{\mathbf{A}_q}-\overline{z}_{\mathbf{A}}\right)\left(u(z_{\mathbf{A}_q})\cos\theta_0-u(z_{\mathbf{A}_p})+(1-\cos\theta_0)u(z_{\mathbf{A}})\right)\Big\}\end{aligned} \tag{S26}$$

Force balance at $\mathbf{A}$ imposes:

$$\sum_p\mathbf{F}_s(\mathbf{A}_p\to\mathbf{A})+\sum_{<p,q>}\mathbf{F}_b(\{\mathbf{A}_p,\mathbf{A}_q\}\to\mathbf{A})=\mathbf{0}, \tag{S27}$$

where p runs over each bond $\mathbf{A}_p$ and $<p,q>$ runs over each bond angle $\widehat{\mathbf{A}_p\mathbf{A}\mathbf{A}}_q$. In the very vicinity of the crack tip and in the limit $L\to\infty$, $u(z)$ only involves two terms: the super-singular ($n=-1$) term due to the tip mispositioning and the singular ($n=1$) term associated with the K-dominant elastic field: $u(z)=a_{-1}\Phi^I_{-1}(z)+a_1\Phi^I_1(z)$. Note that the term $n=0$ is independent of z and corresponds to a constant translation term in the displacement, which has no effect in Eqs. S23 and S26. Equation S27 supplemented with Eqs. S17, S23 and S26 yields:

$$\begin{cases}dS^x_{-1}+2S^x_1=0\\ dS^y_{-1}+2S^y_1=0\end{cases} \tag{S28}$$

with:

$$\begin{aligned}S^x_n = &\sum_p\mathrm{Re}\{(\phi^I_n(z_{\mathbf{A}_p})-\phi^I_n(z_{\mathbf{A}}))(\overline{z}_{\mathbf{A}_p}-\bar{z}_A)\}\,\mathrm{Re}\{z_{\mathbf{A}_p}-z_{\mathbf{A}}\}\\ &+\frac{k_b}{k_s\ell^4\sin\theta_0}\sum_{<p,q>}\mathrm{Im}(\overline{z}_{\mathbf{A}_q}-\overline{z}_{\mathbf{A}_p})\,\mathrm{Im}\{(\overline{z}_{\mathbf{A}_p}-\overline{z}_{\mathbf{A}})(z_{\mathbf{A}_q}-z_{\mathbf{A}})\}\\ &\quad\times\mathrm{Re}\Big\{\left(\overline{z}_{\mathbf{A}_p}-\overline{z}_{\mathbf{A}}\right)\left(\phi^I_n(z_{\mathbf{A}_p})\cos\theta_0-\phi^I_n(z_{\mathbf{A}_q})+(1-\cos\theta_0)\phi^I_n(z_{\mathbf{A}})\right)\\ &\quad\quad+\left(\overline{z}_{\mathbf{A}_q}-\overline{z}_{\mathbf{A}}\right)\left(\phi^I_n(z_{\mathbf{A}_q})\cos\theta_0-\phi^I_n(z_{\mathbf{A}_p})+(1-\cos\theta_0)\phi^I_n(z_{\mathbf{A}})\right)\Big\}\\ S^y_n = &\sum_p\mathrm{Re}\{(\phi^I_n(z_{\mathbf{A}_p})-\phi^I_n(z_{\mathbf{A}}))(\overline{z}_{\mathbf{A}_p}-\bar{z}_A)\}\,\mathrm{Im}\{z_{\mathbf{A}_p}-z_{\mathbf{A}}\}\\ &-\frac{k_b}{k_s\ell^4\sin\theta_0}\sum_{<p,q>}\mathrm{Re}(\overline{z}_{\mathbf{A}_q}-\overline{z}_{\mathbf{A}_p})\,\mathrm{Im}\{(\overline{z}_{\mathbf{A}_p}-\overline{z}_{\mathbf{A}})(z_{\mathbf{A}_q}-z_{\mathbf{A}})\}\\ &\quad\times\mathrm{Re}\Big\{\left(\overline{z}_{\mathbf{A}_p}-\overline{z}_{\mathbf{A}}\right)\left(\phi^I_n(z_{\mathbf{A}_p})\cos\theta_0-\phi^I_n(z_{\mathbf{A}_q})+(1-\cos\theta_0)\phi^I_n(z_{\mathbf{A}})\right)\\ &\quad\quad+\left(\overline{z}_{\mathbf{A}_q}-\overline{z}_{\mathbf{A}}\right)\left(\phi^I_n(z_{\mathbf{A}_q})\cos\theta_0-\phi^I_n(z_{\mathbf{A}_p})+(1-\cos\theta_0)\phi^I_n(z_{\mathbf{A}})\right)\Big\}\end{aligned} \tag{S29}$$

where $n=\{-1,1\}$.

The value of d should satisfy at best Eq. S28. As such, it should minimize the function $f(d)=(dS^x_{-1}+2S^x_1)^2+(dS^y_{-1}+2S^y_1)^2$. Hence, d fulfills $f'(d)=0$, so:

$$d=-2\frac{S^x_{-1}S^x_1+S^y_{-1}S^y_1}{(S^x_{-1})^2+(S^y_{-1})^2} \tag{S30}$$

C. *n order determination of the crack tip mis-positioning*

As in scalar antiplane elastic problem, the above procedure can be improved to reach any prescribed accuracy by (i) imposing force balance to an arbitrary number of atoms and (ii) by applying an iterative procedure to correct mispositioning.

The procedure to account for an arbitrary number of atoms follows the same route as that described in Sec. III. Equation S30 then becomes:

$$d = -2\frac{\sum_{\mathbf{P}}\{S^x_{-1}(z_{\mathbf{P}},z_{\mathbf{P}_i})S^x_1(z_{\mathbf{P}},z_{\mathbf{P}_i}) + S^y_{-1}(z_{\mathbf{P}},z_{\mathbf{P}_i})S^y_1(z_{\mathbf{P}},z_{\mathbf{P}_i})\}}{\sum_{\mathbf{P}}\{(S^x_{-1}(z_{\mathbf{P}},z_{\mathbf{P}_i})^2 + (S^y_{-1}(z_{\mathbf{P}},z_{\mathbf{P}_i})^2\}}, \tag{S31}$$

where $S^{x/y}_n(z_{\mathbf{P}},z_{\mathbf{P}_i})$ are given by Eq. S29. The iterative procedure here mimics that described in Sec. IV.

D. *Subsequent determination of toughness*

Once d has been determined and the true position of the crack tip is known, the value of fracture toughness K_c is deduced, by stating that the stretching applying to the bond $\mathbf{A}-\mathbf{B}$ [Fig. S4(a)] is equal to the bond strength F_c:

$$\|\mathbf{F}_s(\mathbf{B}\to\mathbf{A})\| = \frac{k_s}{\ell}\,\mathrm{Re}\{(u(z_{\mathbf{B}})-u(z_{\mathbf{A}}))(\overline{z}_{\mathbf{B}}-\overline{z}_{\mathbf{A}})\} = F_c \tag{S32}$$

Now that the position of the crack tip is well placed with respect to the frame origin $\mathbf{O}$, and in the limit $L\to\infty$, the displacement at $\mathbf{A}$ and $\mathbf{B}$ are given by:

$$\mathbf{u}(z_{\mathbf{A}}) = \frac{K_c(1+\nu)}{E\sqrt{2\pi}}\Phi^I_1(z_{\mathbf{A}}+d) \quad \text{and} \quad \mathbf{u}(z_{\mathbf{B}}) = \frac{K_c(1+\nu)}{E\sqrt{2\pi}}\Phi^I_1(z_{\mathbf{B}}+d) \tag{S33}$$

where a_1 in Eq. S17 has been replaced by its expression involving K_c in Eq. S20. The expression for K_c follows:

$$K_c = \frac{E\sqrt{2\pi}}{k_s(1+\nu)}\frac{F_c\ell}{\mathrm{Re}\{\left(\Phi^I_1(z_{\mathbf{A}}+d)-\Phi^I_1(z_{\mathbf{B}}+d)\right)(\overline{z}_{\mathbf{A}}-\overline{z}_{\mathbf{B}})\}} \tag{S34}$$

VI. APPLICATION TO GRAPHENE

Graphene is a crystalline allotrope of carbon consisting of a single layer of carbon atoms arranged in a hexagonal lattice of mesh size $\ell = 0.142$ nm [Fig. S4(a)]. Each atom is bonded to its three nearest neighbors via sp2 covalent bonds, so that $\theta_0 \simeq 120°$. The bond stretching stiffness and bond bending stiffness reported in such structures [4] are generally in the range $k_s = 688-740$ N m^{-1} and $k_b = 0.769-0.776\times10^{-18}$ N m rad^{-2}. In addition, there is an additional π-bond oriented out of plane. In such a 2D bidimensional crystal, the position of atom A is $z_{\mathbf{A}} = i\ell/2$ and that of its three nearest-neighbors is $z_{\mathbf{A}_1} = (-2\sqrt{3}/2+i)\ell$, $z_{\mathbf{A}_2} = (2\sqrt{3}/2+i)\ell$ and $z_{\mathbf{A}_3} = -i\ell/2$. Finally, the Poisson ratio is reported to be $\nu = 0.18$. Application of Eq. S30 yields:

$$d[\text{approx.}] \simeq 0.060 \text{ nm} \tag{S35}$$

The application of the iterative procedure (100 iterations) with the most refined Eq. S31 using the first 100$^{\text{th}}$ atoms the closest to frame origin yields:

$$d[\text{exact}] = 0.0934 \text{ nm} \tag{S36}$$

Finally, the application of Eq. S34 with the values $E = 340$ N m^{-1} reported for the Young modulus [5] and $F_c = 13.6$ nN for the bond strength [6] yields:

$$K_c[\text{exact}] = 1.204 \times 10^{-3}\ \text{N}\,\text{m}^{-1/2} \tag{S37}$$

[1] F. Radjai, M. Jean, J.-J. Moreau, and S. Roux, Force distributions in dense two-dimensional granular systems, Physical Review Letters **77**, 274 (1996).

[2] M. L. Williams, Stress singularities resulting from various boundary conditions in angular corners of plates in extension, Journal of Applied Mechanics **19**, 526 (1952).

[3] J. Réthoré and R. Estevez, Identification of a cohesive zone model from digital images at the micron-scale, Journal of the Mechanics and Physics of Solids **61**, 1407 (2013).

[4] J. Medina, F. Avilés, and A. Tapia, The bond force constants of graphene and benzene calculated by density functional theory, Molecular Physics **113**, 1297 (2015).

[5] C. Lee, X. Wei, J. W. Kysar, and J. Hone, Measurement of the elastic properties and intrinsic strength of monolayer graphene, science **321**, 385 (2008).

[6] B. Xu, X. Gao, and Y. Tian, Graphene simulation (InTech, 2011) Chap. Universal Quantification of Chemical Bond Strength and Its application to Low Dimensional Materials, pp. 211–226.